Immunity
Article

The E3 Ubiquitin Ligase Pellino3 Protects against Obesity-Induced Inflammation and Insulin Resistance

Shuo Yang,[1,4] Bingwei Wang,[1,4] Fiachra Humphries,[1] Andrew E. Hogan,[2] Donal O'Shea,[2] and Paul N. Moynagh[1,3,*]
[1]Institute of Immunology, Department of Biology, National University of Ireland Maynooth, Maynooth, Co. Kildare, Ireland
[2]Education and Research Centre, St Vincent's University Hospital, University College Dublin, Dublin 4, Ireland
[3]Centre for Infection and Immunity, School of Medicine, Dentistry and Biomedical Sciences, Queen's University Belfast, Belfast BT9 7AE, Northern Ireland, UK
[4]Co-first author
*Correspondence: paul.moynagh@nuim.ie
http://dx.doi.org/10.1016/j.immuni.2014.11.013

SUMMARY

Diet-induced obesity can induce low-level inflammation and insulin resistance. Interleukin-1β (IL-1β) is one of the key proinflammatory cytokines that contributes to the generation of insulin resistance and diabetes, but the mechanisms that regulate obesity-driven inflammation are ill defined. Here we found reduced expression of the E3 ubiquitin ligase Pellino3 in human abdominal adipose tissue from obese subjects and in adipose tissue of mice fed a high-fat diet and showing signs of insulin resistance. Pellino3-deficient mice demonstrated exacerbated high-fat-diet-induced inflammation, IL-1β expression, and insulin resistance. Mechanistically, Pellino3 negatively regulated TNF receptor associated 6 (TRAF6)-mediated ubiquitination and stabilization of hypoxia-inducible factor 1α (HIF1α), resulting in reduced HIF1α-induced expression of IL-1β. Our studies identify a regulatory mechanism controlling diet-induced insulin resistance by highlighting a critical role for Pellino3 in regulating IL-1β expression with implications for diseases like type 2 diabetes.

INTRODUCTION

There is a strong link between obesity-driven inflammation and insulin resistance and diabetes (Xu et al., 2003). Diet-induced obesity promotes chronic low-grade inflammation as typified by accumulation of M1 macrophages in adipose tissue and enhanced serum concentrations of proinflammatory cytokines (Gregor and Hotamisligil, 2011). This proinflammatory milieu is also associated with hepatic steatosis and ultimately drives peripheral insulin resistance. Multiple innate immune receptors, including members of the Toll-like receptor (TLR) family, have been implicated as triggers of the proinflammatory gene expression that leads to insulin resistance (Jin et al., 2013). Interleukin-1β (IL-1β) is one of the critical proinflammatory cytokines that promotes insulin resistance and diabetes (Tack et al., 2012). The secretion of mature IL-1β requires two signals. First, innate receptors, like toll-like receptor 4 (TLR4), promote increased transcription of the gene encoding IL-1β, resulting in expression of an inactive pro-IL-1β precursor (Skeldon et al., 2014). The transcription of IL-1β is regulated by transcription factors such as nuclear factor-kappa B (NF-κB) and hypoxia inducible factor-1α (HIF-1α) (Baker et al., 2011; Tannahill et al., 2013). A second signal promotes formation of an inflammasome signaling platform containing caspase 1 that processes pro-IL-1β precursor into the mature secreted form of IL-1β (Martinon et al., 2002; Tack et al., 2012). Various molecules, including the saturated fatty acid palmitate, can trigger the second signal to manifest deleterious effects on metabolism and insulin resistance (Wen et al., 2011). Although the IL-1β system has become an important focus for therapeutic intervention in insulin resistance and type 2 diabetes (Böni-Schnetzler and Donath, 2013), the full mechanisms that regulate obesity-driven IL-1β expression and inflammation are ill defined and are of central importance to understanding the pathogenesis of insulin resistance. Here we show an important role for the E3 ubiquitin ligase Pellino3 in regulating diet-induced inflammation and insulin resistance.

Pellino proteins form a family of E3 ubiquitin ligase that play important roles in innate immunity (Moynagh, 2014; Schauvliege et al., 2007). The three members of the Pellino family share a phosphothreonine-binding N-terminal forkhead-associated (FHA) domain and a C-terminal RING-like domain that allow for respective recognition and E3 ligase-mediated ubiquitination of substrate proteins such as interleukin-1 receptor-associated kinase (IRAK) kinases in TLR pathways (Butler et al., 2007; Lin et al., 2008; Ordureau et al., 2008; Schauvliege et al., 2006). The E3 ligase activity of the Pellino proteins is subject to regulation by phosphorylation (Goh et al., 2012; Smith et al., 2009, 2011; Strelow et al., 2003). Genetic models have demonstrated a physiological role for Pellino1 as a mediator of TLR3 and TLR4 signaling (Chang et al., 2009), a negative regulator of T cell activation (Chang et al., 2011; Moynagh, 2011), and a driver of CNS inflammation (Xiao et al., 2013). More recently we have used Pellino3-deficient mice to show that Pellino3 negatively regulates TLR3 signaling and type I interferon (IFN) expression (Siednienko et al., 2012), mediates nucleotide-binding oligomerization domain-containing protein 2 (NOD2) signaling in the

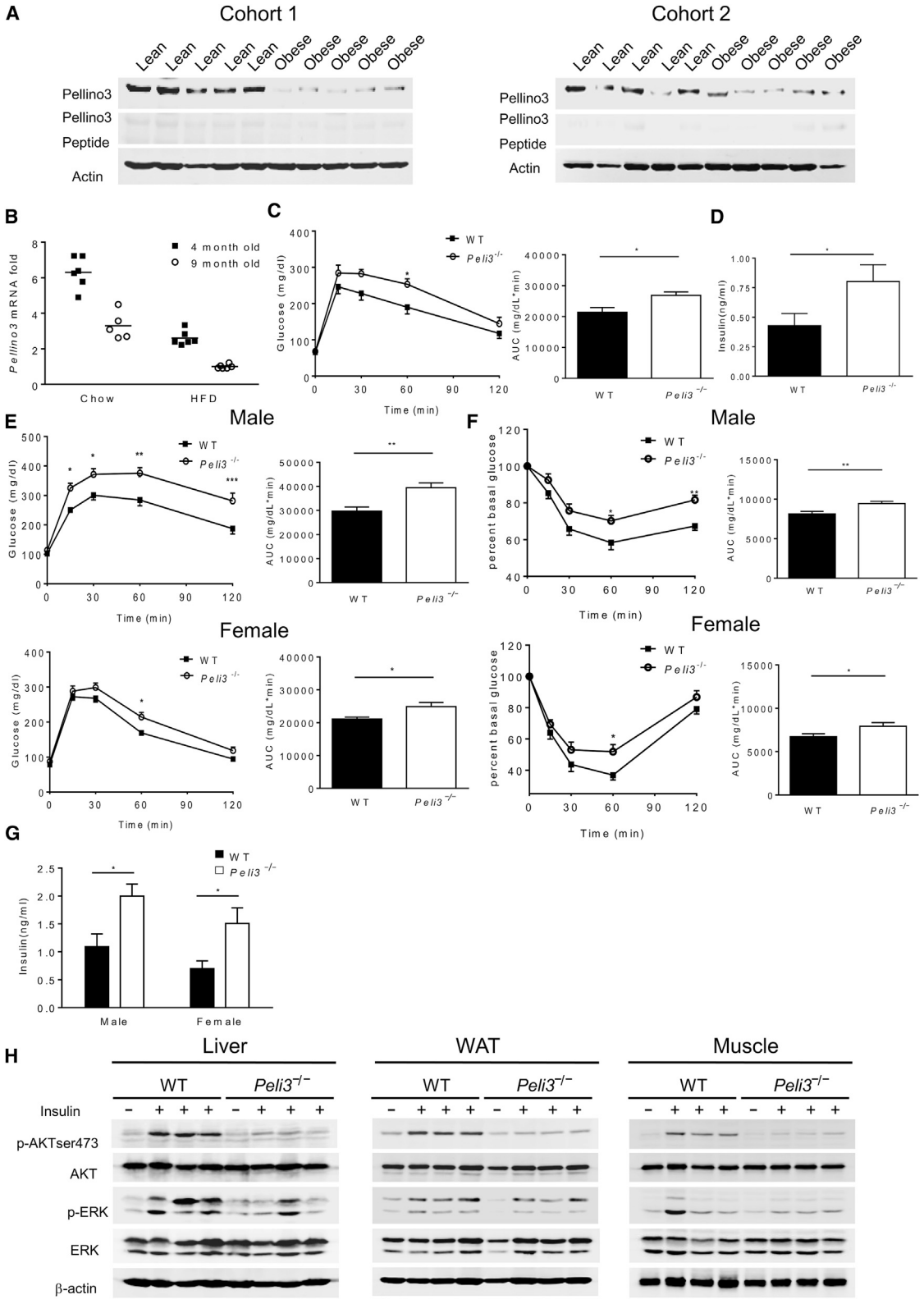

Figure 1. Pellino3 Deficiency Is Associated with Insulin Resistance

(A) Immunoblot analysis of Pellino3 from the abdominal adipose tissue of lean control subjects and patients with obesity. Two separate cohorts of subjects were used for the analysis. Immunoblotting with the anti-Pellino3 antibody was performed in the absence (top) or presence (middle) of the immunogenic peptide that was used to generate the anti-Pellino3 antibody in order to define nonspecific binding of the antibody. Expression of β-actin was used as a loading control.

(legend continued on next page)

intestine (Yang et al., 2013a), and regulates cell killing in response to tumor necrosis factor (TNF) (Yang et al., 2013b). We now demonstrate an important role for Pellino3 in regulating high-fat-diet-induced insulin resistance.

Here we found that Pellino3 expression was greatly reduced in adipose tissue from obese subjects and in mice fed a high-fat diet. Pellino3-deficient mice showed heightened diet-induced inflammation and IL-1β expression that exacerbated insulin resistance. Pellino3 was found to protect against insulin resistance by targeting TRAF6-mediated ubiquitination and stabilization of HIF-1α, thus suppressing expression of HIF-1α-responsive IL-1β. This study thus describes a new mechanism that drives IL-1β expression and highlights Pellino3 as a critical molecule in counteracting this pathway and reducing the risk of developing insulin resistance.

RESULTS

Pellino3 Deficiency Is Associated with Exacerbation of Insulin Resistance

Given the strong links between obesity, inflammation, and insulin resistance, we were keen to assess whether endogenous regulators of the inflammatory response show differential expression in lean and obese adipose tissue. Our recent studies identified important roles for Pellino3 in regulating innate immunity (Siednienko et al., 2012; Yang et al., 2013a, 2013b). In the present study, we initially measured Pellino3 expression in human omental tissue from lean subjects and obese patients. Central abdominal adipose tissue was chosen because there is a strong association between an increase in this type of adipose tissue and insulin resistance (Item and Konrad, 2012; Matsuzawa et al., 1995). The expression of Pellino3 was greatly reduced in omental samples from obese patients (Figure 1A). Reduced expression was also observed in adipose tissue of mice fed a high-fat diet (HFD) (Figure 1B). Decreased expression of Pellino3 was also apparent in aging mice. In order to assess whether decreased Pellino3 expression has functional consequence for insulin sensitivity, a glucose-tolerance test was performed on wild-type and Pellino3-deficient (*Peli3*$^{-/-}$) mice. Loss of Pellino3 associated with reduced glucose tolerance (Figure 1C) and increased serum concentrations of insulin (Figure 1D), suggesting that Pellino3 might be able to regulate metabolic health. This was further confirmed by demonstrating exacerbation of HFD-induced glucose intolerance (Figure 1E), insulin resistance (Figure 1F), and hyperinsulinaemia (Figure 1G) in male and female *Peli3*$^{-/-}$ mice. Furthermore, loss of Pellino3 resulted in impaired insulin signaling in liver, adipose tissue, and muscle, as evidenced by reduced insulin-induced phosphorylation of AKT and ERK in all three tissues from Pellino3-deficient mice (Figure 1H and Figure S1 available online).

We next addressed the underlying basis to the aggravated enhanced insulin resistance in Pellino3-deficient mice. The loss of Pellino3 does not have any major effect on obesity as indicated by the fact that male and female *Peli3*$^{-/-}$ mice show comparable body weights to matched wild-type mice fed normal chow (Figure S2A) and HFD (Figure S2B). Furthermore, HFD wild-type and *Peli3*$^{-/-}$ mice had similar food intake (Figure S2C) and similar sized fat pads apart from some modest increase in the weights of gonadal and inguinal pads from *Peli3*$^{-/-}$ mice (Figure S2D).

Loss of Pellino3 Exacerbates Inflammation in Response to High-Fat Diet

We next characterized the inflammatory status of adipose tissue from HFD Pellino3-deficient mice given that diet-induced obesity and insulin resistance is strongly associated with adipose tissue inflammation (Xu et al., 2003) as typified by accumulation of adipose tissue macrophages, especially proinflammatory M1 macrophages rather than the anti-inflammatory M2 subtype (Lumeng et al., 2007, 2008). Adipose tissue from HFD-fed *Peli3*$^{-/-}$ mice demonstrated much more intense infiltration by leukocytes than similarly fed wild-type mice (Figure 2A), with HFD-induced levels of the M1 *Itgax* and *Nos2* mRNA markers also being higher in *Peli3*$^{-/-}$ mice (Figure 2B). This pattern was also observed in liver samples. The amounts of M2 macrophage-associated *Arg1*, *Mrc1*, *Fizz1*, and *Ym1* mRNA markers were higher in tissues from wild-type mice (Figure 2B), suggesting that lack of Pellino3 favors a heightening of the bias toward accumulation of M1 macrophages in adipose tissue and liver in response to HFD. Flow cytometric analysis, with Cd11c and CD206 as cell surface markers of M1 and M2, respectively (Fujisaka et al., 2009), confirmed that the *Peli3*$^{-/-}$ mice showed greater accumulation of adipose tissue M1 macrophages but lower numbers of M2 macrophages (Figure 2C). Pellino3 was also examined for a potential cell-intrinsic role in regulating macrophage polarization. Thus, M-CSF-cultured macrophages from bone marrow of wild-type and *Peli3*$^{-/-}$ mice were stimulated with LPS and IFN-γ or IL-4 and IL-10 to generate in vitro M1 and M2 populations, respectively (Figure S3A). Flow cytometric analysis, with M1 and M2 markers, demonstrated that M-CSF-cultured macrophages from *Peli3*$^{-/-}$ mice showed greater expression of the M1 marker CD86, in response to LPS and IFN-γ, than similarly treated cells from wild-type mice, whereas the induction of the M2 marker CD206 was

(B) Quantitative PCR of mRNA expression for *Pellino3* in epididymal fat pad isolated from mice fed ad libitum a chow diet (18% fat) or high-fat diet (HFD) (60% fat), starting at 2 months of age for all groups and continued for an additional 2 or 7 months (n = 5–6).
(C and D) Glucose-tolerance test (GTT) (left) and the total area under the curve (AUC) analysis (right) for GTT (C) and ELISA analysis of insulin expression in serum (D) from 10-month-old wild-type (WT) and *Peli3*$^{-/-}$ mice fed a chow diet (n = 9; *p < 0.05).
(E and F) GTT and AUC analysis (E) and insulin-tolerance test (ITT) and AUC analysis (F) in 6-month-old male (top) and female (bottom) WT and *Peli3*$^{-/-}$ mice fed a HFD from 2 months old (n = 11–14; *p < 0.05; **p < 0.01).
(G) ELISA analysis of insulin expression in serum from 6-month-old WT and *Peli3*$^{-/-}$ mice fed a HFD from 2 months old (n = 13–14, *p < 0.05). All data are presented as the mean ± SEM and were subjected to two-way ANOVA analysis, followed by Bonferroni's multiple-comparison test or to unpaired Student's t test.
(H) Immunoblot analysis of phosphorylated (p-) and total AKT and ERK in liver, white adipose tissue (WAT), and muscle from 6-month-old WT and *Peli3*$^{-/-}$ mice, left untreated (–) or after insulin (1 U/kg) injection (+) for 8 min. Mice were fed a HFD from 2 months old. β-actin was used as a loading control.
See also Figure S1.

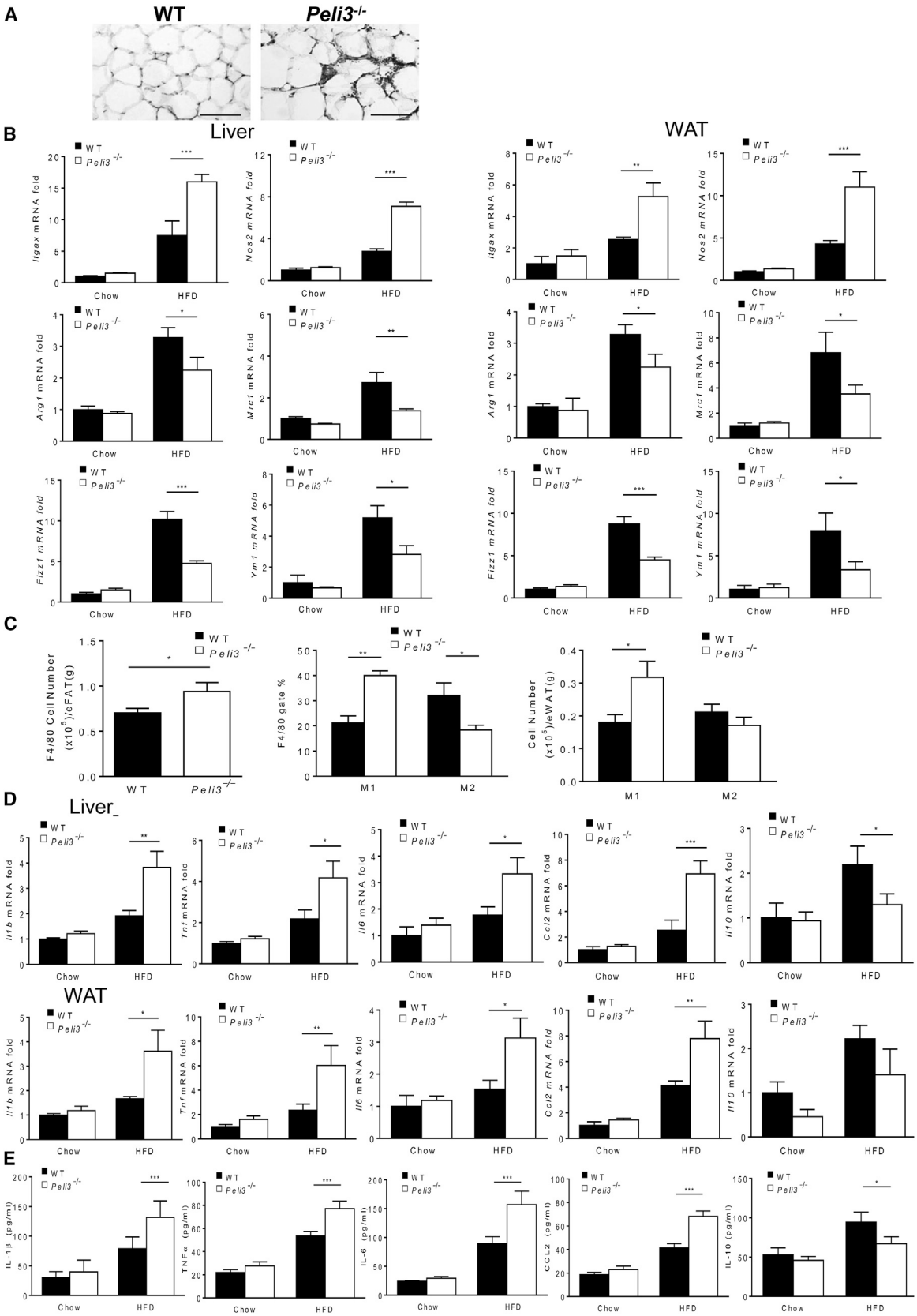

(legend on next page)

comparable in IL-4- and IL-10-treated macrophages from wild-type and *Peli3*$^{-/-}$ mice (Figure S3B). Furthermore, LPS and IFN-γ induced more M1-associated *Nos2*, *Il1b*, and *Tnf* mRNA in macrophages from *Peli3*$^{-/-}$ mice whereas IL-4 and IL-10 induced similar expression of M2-associated *Arg1*, *Fizz1*, and *Il10* mRNA in cells from wild-type and *Peli3*$^{-/-}$ mice (Figure S3C). These findings suggest that Pellino3 has a cell-intrinsic role in negatively regulating macrophage M1 polarization but does not directly influence the generation of M2 macrophages. The lower number of adipose tissue M2 macrophages in HFD-fed *Peli3*$^{-/-}$ mice might be secondary to the strong M1 inflammatory microenvironment. The lack of direct effect of Pellino3 in M2 polarization is also consistent with chow-fed wild-type and *Peli3*$^{-/-}$ mice showing similar number of peritoneal macrophages (Figure S3D), because macrophages isolated from the peritoneum have previously been shown to display a M2-type phenotype (Takeda et al., 2010).

The greater number of inflammatory M1 cells in the adipose tissue and liver of Pellino3-deficient mice was associated with higher HFD-induced tissue expression of the inflammatory mRNAs *Il1b*, *Tnf*, *Il6*, and *Ccl2* but lower amounts of anti-inflammatory *Il10* mRNA in *Peli3*$^{-/-}$ mice relative to wild-type mice (Figure 2D). The HFD-fed *Peli3*$^{-/-}$ mice also displayed higher HFD-induced serum concentrations of the proinflammatory cytokines (Figure 2E), suggesting that Pellino3 can limit the magnitude of the inflammatory response in liver and adipose tissue in response to HFD. Because hepatic steatosis and liver injury are key features associated with obesity-driven inflammation and are likely key contributors to insulin resistance (Asrih and Jornayvaz, 2013), we also compared liver samples from wild-type and *Peli3*$^{-/-}$ mice fed a HFD. Both types of mice showed clear signs of hepatic steatosis but pathology was exacerbated in *Peli3*$^{-/-}$ mice as evidenced by more pronounced hepatocyte ballooning and empty vacuoles in histological analysis of liver samples from mice lacking Pellino3 (Figure 3A). The propensity of *Peli3*$^{-/-}$ mice to more severe steatosis is further supported by the fact that these mice expressed higher hepatic levels of the genes *Fsn* and *Acaca*, which promote fatty acid biosynthesis, but lower levels of *Cpt1a* that initiates mitochondrial β-oxidation of fatty acids (Figure 3B). In addition, HFD-fed *Peli3*$^{-/-}$ mice also showed higher serum concentrations of triglycerides than wild-type mice on the same diet (Figure 3C). Taken together these data strongly support a role for Pellino3 in limiting the extent of obesity-driven inflammation and in protecting against hepatic steatosis and insulin resistance.

Pellino3 Deficiency Results in Enhanced Expression of IL-1β that Drives Insulin Resistance

We next addressed the molecular mechanism underlying the hyperinflammatory response in HFD-fed *Peli3*$^{-/-}$ mice and explored whether this heightened inflammation drives the more severe insulin resistance observed in these mice. Although the exact triggers of obesity-driven inflammation that leads to insulin resistance remain to be defined, various Toll-like receptors (TLRs) have been proposed to play roles (Könner and Brüning, 2011) with particular focus on TLR4 (Poggi et al., 2007; Tsukumo et al., 2007). TLR4 can be stimulated by LPS, whose circulating levels increase in obesity (Baker et al., 2011), and by free fatty acids to trigger inflammatory cytokine expression and insulin resistance (Nguyen et al., 2007). To this end we used bone-marrow-derived macrophages from wild-type and *Peli3*$^{-/-}$ mice and compared their inflammatory responses to treatment with LPS and the saturated fatty acid palmitate. LPS induced the expression of IL-1β, TNF, IL-6, IL-10, IL-12, CCL5, CXCL1, and CCL2 to the same extent in wild-type and *Peli3*$^{-/-}$ bone-marrow-derived macrophages (BMDMs) (Figures 4A and S4). Palmitate alone induced no detectable levels of cytokines but notably strongly augmented the LPS-induced expression of IL-1β while having no effects on the other cytokines (Figure 4A). Induction of IL-1β in response to LPS and palmitate was further enhanced in *Peli3*$^{-/-}$ BMDMs relative to wild-type cells whereas all other cytokines were expressed in similar amounts between wild-type and *Peli3*$^{-/-}$ cells. Given the very selective targeting of IL-1β expression by Pellino3, coupled to the previously described roles for IL-1β in insulin resistance (Tack et al., 2012), we assessed whether the exacerbation of HFD-induced insulin resistance in *Peli3*$^{-/-}$ mice was directly attributable to IL-1β. Glucose- and insulin-tolerance tests demonstrated that administration of IL-1 receptor antagonist reversed insulin resistance in *Peli3*$^{-/-}$ mice, resulting in restoration of insulin sensitivity and glucose tolerance to these mice (Figure 4B). The IL-1 receptor antagonist improved glucose homeostasis in *Peli3*$^{-/-}$ mice without affecting weight, suggesting that the effects of the antagonist are not secondary to regulation of obesity (Figure 4C). These data confirm that the augmented expression of IL-1β in *Peli3*$^{-/-}$ cells is a critical and direct contributory factor to driving the insulin-resistance phenotype and we therefore probed the mechanism by which Pellino3 regulates IL-1β expression.

The production and release of IL-1β requires two signals: the first signal induces transcription of *Il1b* and expression of precursor pro-IL-1β and the second signal activates the inflammasome to trigger caspase1-mediated processing of pro-IL-1β into

Figure 2. Pellino3 Deficiency Exacerbates Inflammation in Response to HFD

(A) H&E staining of sections of epididymal adipose tissue from 6-month old wild-type and *Peli3*$^{-/-}$ mice fed a HFD from 2 months old. Scale bars represent 25 μm.

(B) Quantitative RT-PCR of mRNA expression for *Itgax*, *Nos2*, *Arg1*, *Mrc1*, *Fizz1*, and *Ym1* in the liver and white adipose tissue (WAT) of 6-month-old wild-type (WT) and *Peli3*$^{-/-}$ mice fed a normal chow diet or HFD from 2 months old (n = 6).

(C) FACS analysis of F4/80-positive stromal vascular fraction (SVF) cell number (left) and the frequency (middle) and number (right) of M1 and M2 macrophage in F4/80-positive SVF from 1 g of epididymal fat tissue taken from 6-month-old WT and *Peli3*$^{-/-}$ mice fed a HFD from 2 months old. F4/80^{+}CD11c^{+}CD206^{-} cells counted as M1 macrophages and F4/80^{+}CD11c^{-}CD206^{+} cells counted as M2 macrophages (n = 9 per group).

(D) Quantitative RT-PCR of mRNA expression for *Il1b*, *Tnf*, *Il6*, *Ccl2*, and *Il10* in the liver (top) and WAT (bottom) of 6-month-old WT and *Peli3*$^{-/-}$ mice fed a chow diet or HFD from 2 months old (n = 6 per group).

(E) ELISA analysis of IL-1β, TNF, IL-6, CCL2, and IL-10 expression in serum from 6-month-old WT and *Peli3*$^{-/-}$ mice fed a chow diet or HFD from 2 months old (n = 9–12).

Data are presented as the mean ± SEM and were subjected to two-way ANOVA analysis, followed by Bonferroni's multiple-comparison test. *p < 0.05, **p < 0.01, ***p < 0.001. See also Figures S2 and S3.

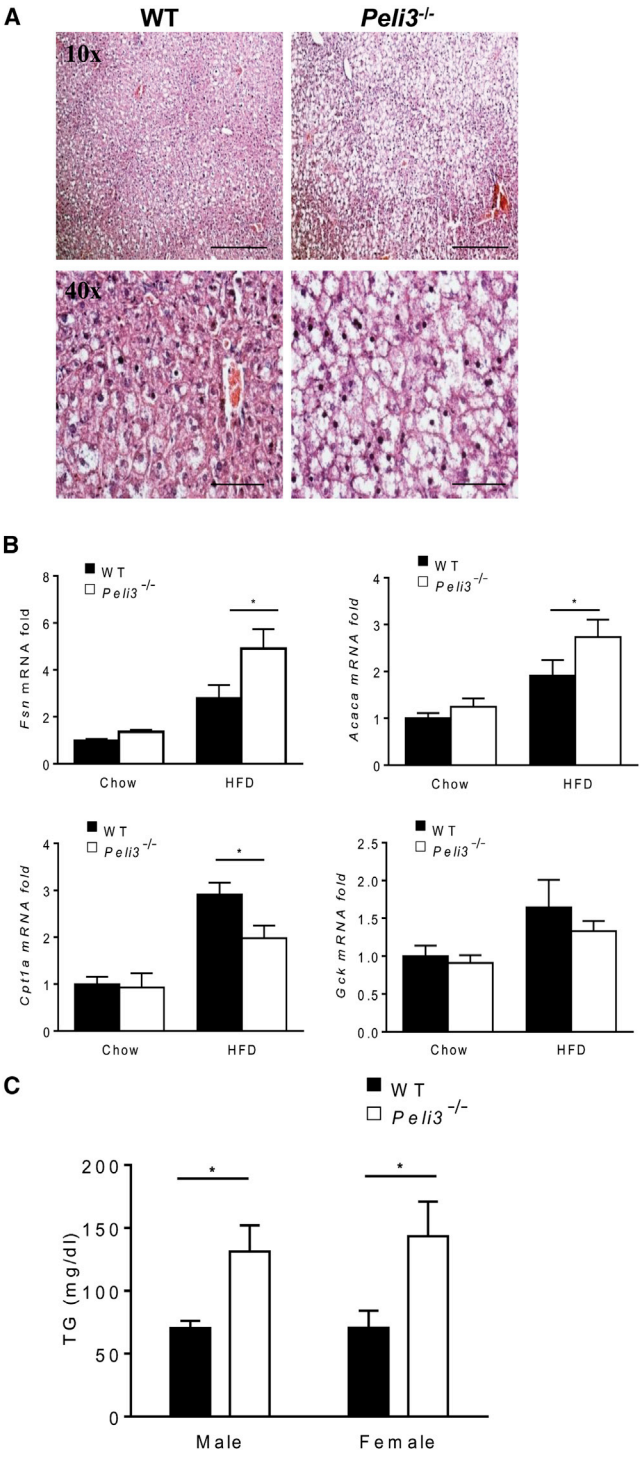

Figure 3. Pellino3 Deficiency Exacerbates Hepatic Steatosis in Response to High-Fat Diet

(A) Hematoxylin and eosin (H&E) staining of liver sections from 6-month-old wild-type and *Peli3*$^{-/-}$ mice fed a HFD from 2 months old. Scale bars represent 25 μm (top) and 100 μm (bottom).

(B) Quantitative PCR of mRNA expression for *Fsn*, *Acaca*, *Cpt1a*, and *GCK* in the liver from 6-month-old wild-type and *Peli3*$^{-/-}$ mice fed a HFD from 2 months old. Data are presented as the mean ± SEM and were subjected to two-way ANOVA analysis, followed by Bonferroni's multiple-comparison test. *$p < 0.05$.

(C) Serum concentrations of triglyceride (TG) from 6-month-old wild-type and *Peli3*$^{-/-}$ mice fed a HFD from 2 months old. Mice were fasted overnight before blood collection (n = 11–14 per group).

mature IL-1β that is secreted from the cell. We therefore subjected adipose tissue from HFD-fed wild-type and *Peli3*$^{-/-}$ mice to immunoblotting and measured the amount of pro-IL-1β and mature IL-1β and found that the amounts of both forms were higher in adipose tissue from *Peli3*$^{-/-}$ mice (Figure 4D). This suggested that Pellino3 targets the initial expression of pro-IL-1β. This was confirmed by LPS and palmitate inducing higher levels of *Il1b* mRNA from 12 hr in *Peli3*$^{-/-}$ BMDMs relative to wild-type cells, indicating that Pellino3 regulates the transcription of IL-1β (Figure 4E). Again this regulatory effect is selective for expression of IL-1β: loss of Pellino3 had no major effect on the LPS-and-palmitate-induced expression of mRNAs encoding IL-6 and TNF (Figure 4E).

Pellino3 Negatively Regulates the Stability of HIF-1α Protein

In order to probe the mechanism by which Pellino3 affects transcriptional regulation of IL-1β, we examined its potential role in regulating activation of NF-κB and HIF-1α, two transcription factors that are known to drive transcription of IL-1β (Baker et al., 2011; Tannahill et al., 2013). LPS and palmitate promoted similar profiles of time-dependent activation of NF-κB in wild-type and *Peli3*$^{-/-}$ BMDMs as measured by phosphorylation of IκBα (Figure 5A) and its upstream kinases IKKα and IKKβ (Figure S5). LPS or LPS and palmitate costimulation resulted in increased amounts of HIF-1α in wild-type cells, which were further increased in *Peli3*$^{-/-}$ BMDMs (Figure 5A), suggesting that Pellino3 targets the HIF-1α pathway. The enhanced expression of HIF-1α in *Peli3*$^{-/-}$ BMDMs are especially evident at later times after LPS stimulation (e.g., 6–12 hr), and this is associated with augmented IL-1β expression at 12–24 hr (Figure 5A, left panels). The regulation of LPS and palmitate signaling by Pellino3 appears to be selective for HIF-1α because lack of Pellino3 does not affect the ability of these stimuli to activate other pathways such as the p38 (Figure 5A) and JNK MAPKs (Figure S5). Given the selective targeting of HIF-1α by Pellino3, we then measured HIF-1α protein in tissues from *Peli3*$^{-/-}$ mice and demonstrated higher protein expression of HIF-1α protein in liver and adipose tissue from *Peli3*$^{-/-}$ mice relative to the same tissues from wild-type mice (Figure 5B). This is consistent with the higher expression of IL-1β in *Peli3*$^{-/-}$ mice and supports a role for Pellino3 in targeting HIF-1α to control expression of IL-1β. We next investigated the molecular basis of the regulatory effects of Pellino3 on HIF-1α. Pellino3 fails to affect the transcription of the gene encoding HIF-1α as shown by the fact that LPS and palmitate induced comparable *Hif1a* mRNA in BMDMs from wild-type and from *Peli3*$^{-/-}$ mice (Figure 5C). Under the same conditions, *Peli3*$^{-/-}$ BMDMs show higher LPS-and-palmitate-induced expression of *Vegf*, another HIF-1α-responsive gene, further confirming the regulatory effects of Pellino3 on HIF-1α (Figure 5C). The levels of *Hif1a* mRNA in liver and adipose tissue are the same in wild-type and *Peli3*$^{-/-}$ mice although the expression of another HIF-1α-responsive gene, *Pdk1*, is increased in tissues from *Peli3*$^{-/-}$ mice (Figure 5D), confirming that Pellino3 targets HIF-1α but posttranscriptionally. Such targeting of

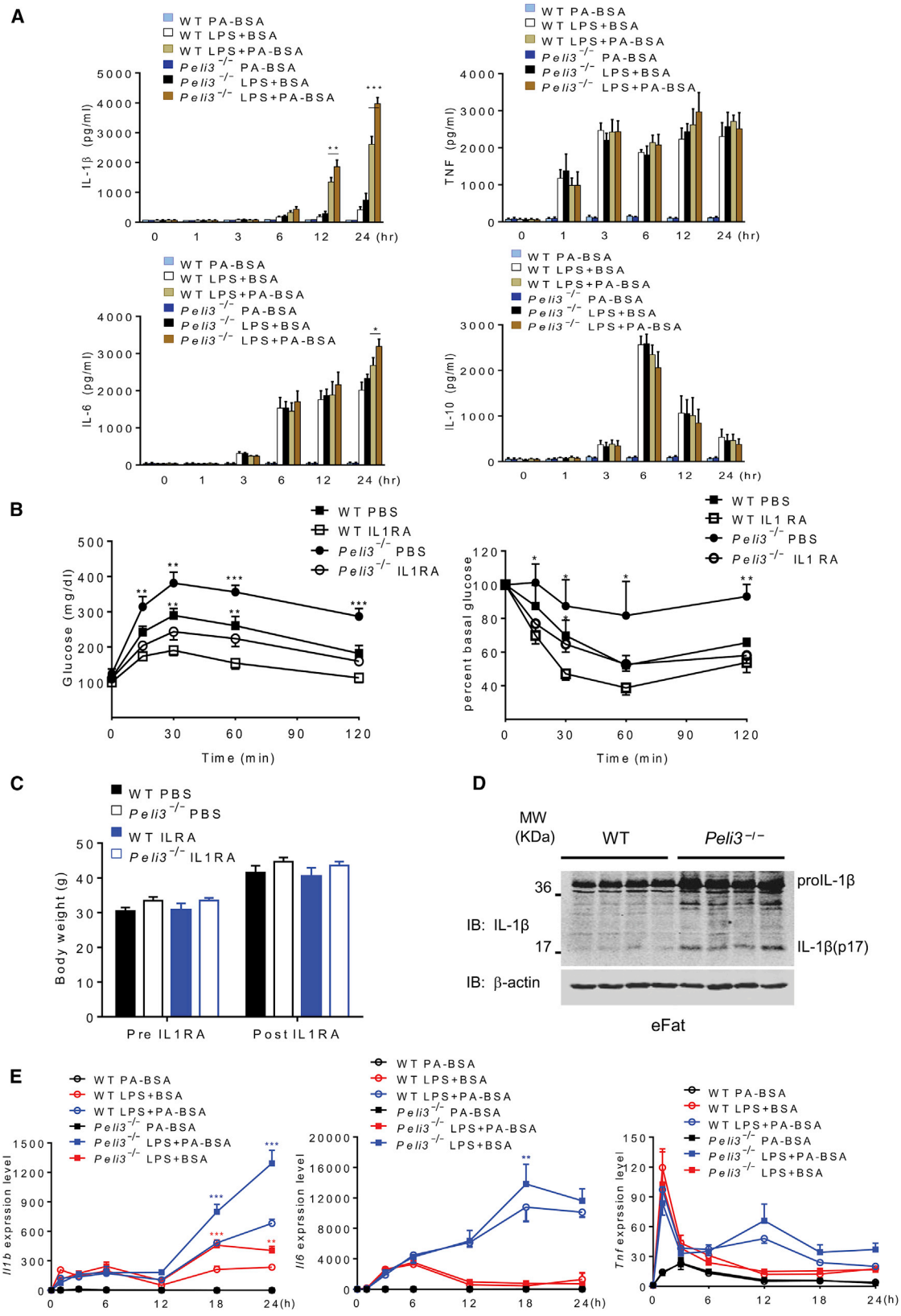

(legend on next page)

HIF-1α by Pellino3 is likely to make an important contribution to the protective effects of Pellino3 in insulin resistance because HIF-1α has been shown to contribute to HFD-induced inflammation and insulin resistance (Jiang et al., 2011; Kihira et al., 2014; Lee et al., 2014; Shin et al., 2012). Indeed, HIF-1α is increased during M1 but not M2 macrophage polarization (Takeda et al., 2010), with HIF-1α being important for mediating expression of proinflammatory cytokines, including IL-1β, in adipose tissue M1 macrophages but dispensable for expression of M2 marker proteins (Fujisaka et al., 2013). Given that we demonstrated above (Figure S3) that Pellino3 plays a cell-intrinsic role in regulating M1 but not M2 macrophage polarization, we measured HIF-1α and IL-1β protein expression in in-vitro-polarized M1 and M2 macrophages from wild-type and *Peli3*$^{-/-}$ mice (Figure 5E). As expected, costimulation of wild-type macrophages with LPS and IFN-γ induced strong expression of the M1 marker protein NOS2, and this was also accompanied by induction of HIF-1α and IL-1β. The protein expression of NOS2, HIF-1α, and IL-1β, in response to LPS and IFN-γ, was further augmented in M1 macrophages from *Peli3*$^{-/-}$ mice. In contrast, IL-4 and IL-10 induced comparable expression of the M2 marker protein, arginase 1, in macrophages from wild-type and *Peli3*$^{-/-}$ mice and failed to induce HIF-1α or IL-1β (Figure 5E). The M1-inducing stimuli of LPS and IFN-γ increased mRNA expression of *Hif1a* in macrophages from wild-type mice but these were not further enhanced in macrophages from *Peli3*$^{-/-}$ mice (Figure 5F). These findings support a model in which Pellino3 can target HIF-1α expression posttranscriptionally to negatively regulate generation of M1 macrophages and the expression of proinflammatory cytokines such as IL-1β.

We next focused our studies on the potential regulatory effects of Pellino3 on the stability of the HIF-1α protein. Under normoxic conditions, newly synthesized HIF-1α is labile by virtue of being subject to proline hydroxylation by three prolyl hydoxylases (PHDs), resulting in interaction with von-Hippel-Lindau (VHL) protein that recruits an elongin B-elongin C-cullin-2-ring box-1-containing E3 ubiquitin ligase complex that targets the hydroxylated HIF-1α for polyubiquitination and proteasomal degradation (Jaakkola et al., 2001; Ohh et al., 2000). Under hypoxic conditions, the oxygen-requiring PHDs are inhibited and the reduced hydroxylation of HIF-1α prevents VHL recognition and thus stabilizes HIF-1α by sparing it from ubiquitination and degradation. Hypoxia is also of particular relevance to obesity and insulin resistance because adipocyte hypertrophy in obese situations leads to hypoxia in the adipose tissue, and it has been proposed that such oxygen deficiency is a key trigger for low inflammation that leads to insulin resistance (Hodson, 2014; Lee et al., 2014; Regazzetti et al., 2009). We therefore explored the regulatory role of Pellino3 in hypoxia-mediated stabilization of HIF-1α protein and demonstrated that the absence of Pellino3 in *Peli3*$^{-/-}$ BMDMs resulted in enhanced HIF-1α protein in response to hypoxic challenge (5% O_2) (Figure 6A). This is also consistent with hypoxic conditions inducing higher expression of the HIF-1α-responsive genes *Il1b*, *Itgax*, *Pdk1*, and *Vegf* in *Peli3*$^{-/-}$ BMDMs while the expression of other genes such as *Tnf*, *Il10*, and *Hif1a* itself were the same in wild-type and *Peli3*$^{-/-}$ cells (Figure 6B). LPS and hypoxia showed strong synergistic effects on stabilization of HIF-1α protein and this was further augmented in *Peli3*$^{-/-}$ cells (Figure 6A). Treatment of cells with the proteasome inhibitor MG132 caused expected accumulation of HIF-1α protein under normoxia and hypoxia with no differences between wild-type and *Peli3*$^{-/-}$ cells (Figure 6C), indicating that Pellino3 affects the pathway that promotes HIF-1α degradation. We next used two PHD inhibitors, dimethyloxalylglycine (DMOG) and cobalt chloride (Figure S6A), to stabilize HIF-1α protein, and with both inhibitors the stabilized expression was similar in wild-type and *Peli3*$^{-/-}$ cells, suggesting that hydroxylation of HIF-1α protein is required to observe the regulatory effects of Pellino3. However, Pellino3 does not affect the hydroxylation of HIF-1α protein (Figure S6B), suggesting that Pellino3 targets events after HIF-1α hydroxylation. Under all of the above conditions of normoxia and hypoxia, in the absence and presence of PHD and proteasome inhibitors, the loss of Pellino3 had no effect on the expression of PHD1-3 or the VHL, elongin B, and elongin C components of the E3 ligase complex that targets HIF-1α for degradation (Figures 6C and S6A). In addition, the absence of Pellino3 had no effect on the assembly of the VHL-elongin B-elongin C-cullin-2-ring box-1 complex (Figure S6C).

We then characterized the ubiquitination status of HIF-1α. As expected, in wild-type cells HIF-1α showed high amounts of degradative-type K48-linked polyubiquitination under normoxic conditions and this was reduced in hypoxia (Figure 6D). K48-linked ubiquitination of HIF-1α was greatly suppressed in *Peli3*$^{-/-}$ cells under both normoxic and hypoxic conditions, suggesting that Pellino3 facilitates K48-linked ubiquitination of HIF-1α. The decreased K48-linked polyubiquitination of HIF-1α in *Peli3*$^{-/-}$ cells was conversely associated with high amounts of nondegradative K63-linked polyubiquitination of HIF-1α (Figure 6D), especially under hypoxic conditions, suggesting that HIF-1α might be subject to competition for ubiquitination by K48- and K63-linked chains resulting in HIF-1α degradation or stabilization, respectively. The increased K63-linked polyubiquitination of HIF-1α, with coincident reduction in K48-linked polyubiquitination, was also observed in *Peli3*$^{-/-}$ cells that were treated with LPS and palmitate (Figure 6E). Such findings suggest that under hypoxic or inflammatory conditions, Pellino3

Figure 4. Pellino3 Targets the Expression of IL-1β to Regulate Insulin Resistance

(A) ELISA analysis of IL-1β, TNF, IL-6, and IL-10 expression in media from bone-marrow-derived macrophages (BMDMs) isolated from WT and *Peli3*$^{-/-}$ mice and treated for 0–24 hr with BSA (400 μM) or palmitate conjugated to BSA (PA-BSA) (400 μM) in the absence or presence of LPS (100 ng/ml).

(B and C) Glucose-tolerance test (GTT) (B, left) and insulin-tolerance test (ITT) (B, right) and body weights (C) of 6-month-old male WT and *Peli3*$^{-/-}$ mice fed a HFD from 2 months old, and intraperitoneally injected with PBS or IL-1 receptor antagonist (IL-1RA; 10 mg/kg) each day from 12 weeks of age for 12 weeks (n = 5).

(D) Immunoblot analysis of IL-1β in epididymal fat tissue from 7-month-old WT and *Peli3*$^{-/-}$ mice fed a HFD from 2 months old. Precursor (pro) and active processed forms of IL-1β (p17) are indicated.

(E) Quantitative RT-PCR of mRNA expression for *Il1b*, *Il6*, and *Tnf* in BMDMs isolated from WT and *Peli3*$^{-/-}$ mice and treated for 0–24 hr with BSA or PA-BSA in the absence or presence of LPS.

All data are presented as the mean ± SEM of three or four independent experiments and were subjected to two-way ANOVA analysis, followed by Bonferroni's multiple-comparison test. *$p < 0.05$, **$p < 0.01$, ***$p < 0.001$. See also Figure S4.

positively regulates K48 ubiquitination of HIF-1α and negatively affects its K63 ubiquitination, thus favoring degradation of HIF-1α. Notably, Pellino3 is not a direct E3 ligase for HIF-1α (Figure 6F), suggesting that the effects of Pellino3 on HIF-1α are indirect in nature.

Pellino3 Targets TRAF6-Mediated Ubiquitination and Stabilization of HIF-1α

Our efforts next focused on how Pellino3 can indirectly regulate the ubiquitination of HIF-1α. We previously showed that Pellino3 can negatively regulate the E3 ubiquitin ligase TRAF6 (Siednienko et al., 2012) and the latter has recently been implicated as an E3 ligase of HIF-1α to promote its K63-linked ubiquitination and stabilization (Sun et al., 2013). Therefore, we hypothesized that Pellino3 might negatively regulate the competing pathway of K63-linked ubiquitination of HIF-1α. The K63-linked polyubiquitination of HIF-1α (Figure 7A) and overall expression of HIF-1α (Figure 7B) were greatly reduced in TRAF6-deficient cells under normoxic and hypoxic conditions. Reconstitution of *Traf6*$^{-/-}$ cells with wild-type TRAF6, but not a C70A point mutant form that lacks E3 ligase activity, resulted in restoration to normal expression of HIF-1α (Figure 7C). TRAF6 is known to be subject itself to ubiquitination at K124, and interestingly a point mutation of TRAF6 (K124A), which abrogates ubiquitination of TRAF6, is more effective than wild-type TRAF6 in elevating HIF-1α expression (Figure 7C), suggesting that ubiquitination of TRAF6 negatively regulates its ability to stabilize HIF-1α. We demonstrate that Pellino3 promotes ubiquitination of TRAF6 because *Peli3*$^{-/-}$ cells show less ubiquitination of TRAF6 than wild-type cells under normoxia and hypoxia (Figure 7D) and in response to stimulation with LPS and palmitate (Figure 7E). This is consistent with the enhanced expression of HIF-1α that was observed under these conditions in Pellino3-deficient cells. We next explored how Pellino3-induced ubiquitination of TRAF6 can regulate the effects of TRAF6 on HIF-1α. Hypoxia promoted increased interaction of TRAF6 with HIF-1α and Pellino3 (Figure 7F), but the TRAF6-HIF-1α association was greatly enhanced in *Peli3*$^{-/-}$ cells (Figure 7G), suggesting that Pellino3-mediated ubiquitination of TRAF6 serves to inhibit the interaction of the latter with HIF-1α. This is fully consistent with overexpression of Pellino3, but not a RING domain mutant form that lacks E3 ligase activity (Yang et al., 2013a), abrogating the ability of TRAF6 to promote K63-linked ubiquitination of HIF-1α (Figure 7H). Pellino3 also contains a phosphothreonine-binding FHA domain, but mutation of this site does not affect the ability of Pellino3 to bind TRAF6 (Figure S7) or regulate TRAF6-induced ubiquitination of HIF-1α (Figure 7H). The negative effects of Pellino3 on TRAF6-mediated ubiquitination of HIF-1α probably underlies the ability of Pellino3, but not its RING domain mutant form, to reduce expression of HIF-1α, under hypoxic conditions, in wild-type cells (Figure 7I). Notably, Pellino3 fails to affect HIF-1α expression in *Traf6*$^{-/-}$ cells (Figure 7I), confirming the dependency of TRAF6 for manifesting the regulatory effects of Pellino3. Finally, we used coexpression studies to directly demonstrate that Pellino3 inhibits the ability of wild-type TRAF6 to stabilize HIF-1α but not the stabilizing effects of the K124A TRAF6 mutant that is resistant to ubiquitination (Figure 7J). This supports our overall model that Pellino3-mediated ubiquitination of TRAF6 is a critical step in negatively regulating the interaction of TRAF6 with HIF-1α, resulting in decreased K63-linked ubiquitination and destabilization of HIF-1α.

DISCUSSION

Obesity-driven inflammation is stongly associated with insulin resistance and IL-1β is a central driver of the low-level inflammation that can lead ultimately to diabetes. Given such damaging consequences of IL-1β, it is vitally important that the body is equipped with regulatory systems to control this unwanted activity and avoid pathology. Most studies to date have focused on inflammasome-mediated processing of the inactive precursor pro-IL-1β to mature IL-1β as a key regulatory checkpoint in the production of IL-1β (Tack et al., 2012). We now propose a major role and signaling axis for the arm of the pathway that drives the transcription of the IL-1β gene. We show that inflammatory and/or hypoxic conditions can employ TRAF6 to ubiquitinate and stabilize HIF-1α and drive IL-1β expression. Pellino3 is shown to be a negative regulator of this pathway by ubiquitinating TRAF6 and so inhibiting the ability of the latter to interact with and stabilize HIF-1α, resulting in suppression of IL-1β expression and protection against insulin resistance. The targeting of TRAF6 by Pellino3 is especially intriguing given our recent study that showed Pellino3 to inhibit TLR3-induced expression of type I interferons by promoting ubiquitination of TRAF6, thus precluding interaction of the latter with IRF7 (Siednienko et al., 2012). This leads to reduced ubiquitination of IRF7, resulting in less nuclear translocation and reduced type I interferon expression. In the present study, Pellino3 ubiquitinates TRAF6 with lysine 63-linked polyubiquitin chains to block the interaction of TRAF6 with HIF-1α. This results in reduced lysine 63-linked polyubiquitination of HIF-1α, making it more susceptible to lysine 48-linked polyubiquitination and proteasomal degradation. These findings propose an emerging paradigm of Pellino3 ubiquitinating TRAF6 to impair binding of the latter to effector molecules and so suppress or terminate downstream signaling and limit cytokine expression.

The study further emphasizes the intrinsic link between obesity, inflammation, and insulin resistance. Pellino3-deficient mice, which show aggravated insulin resistance in response to high-fat diet, bear all the hallmarks of low-grade chronic inflammation that is typical of obesity-driven insulin resistance. The mice show enhanced M1 macrophage accumulation in adipose and liver tissue, with the latter also demonstrating clear signs of severe steatosis. In addition, Pellino3 seems to target HIF-1α to negatively regulate the generation of M1 macrophages and the expression of proinflammatory cytokines such as IL-1β, at least in an in vitro setting. Pellino3-deficient mice also express higher amounts of proinflammatory cytokines in both adipose and liver tissue and serum. However, the enhanced levels of proinflammatory IL-1β appears to be the critical factor in driving insulin resistance in Pellino3-deficient mice by virtue of insulin sensitivity being restored in response to administration of the IL-1 receptor antagonist.

We also highlight the importance of hypoxia and the transcription factor HIF-1α in driving IL-1β expression. Such factors probably play key contributing roles in the generation of insulin resistance. Obesity is associated with adipocyte hypertrophy that results in hypoxia in the adipose tissue, thus promoting inflammation and insulin resistance (Hodson, 2014; Lee et al., 2014;

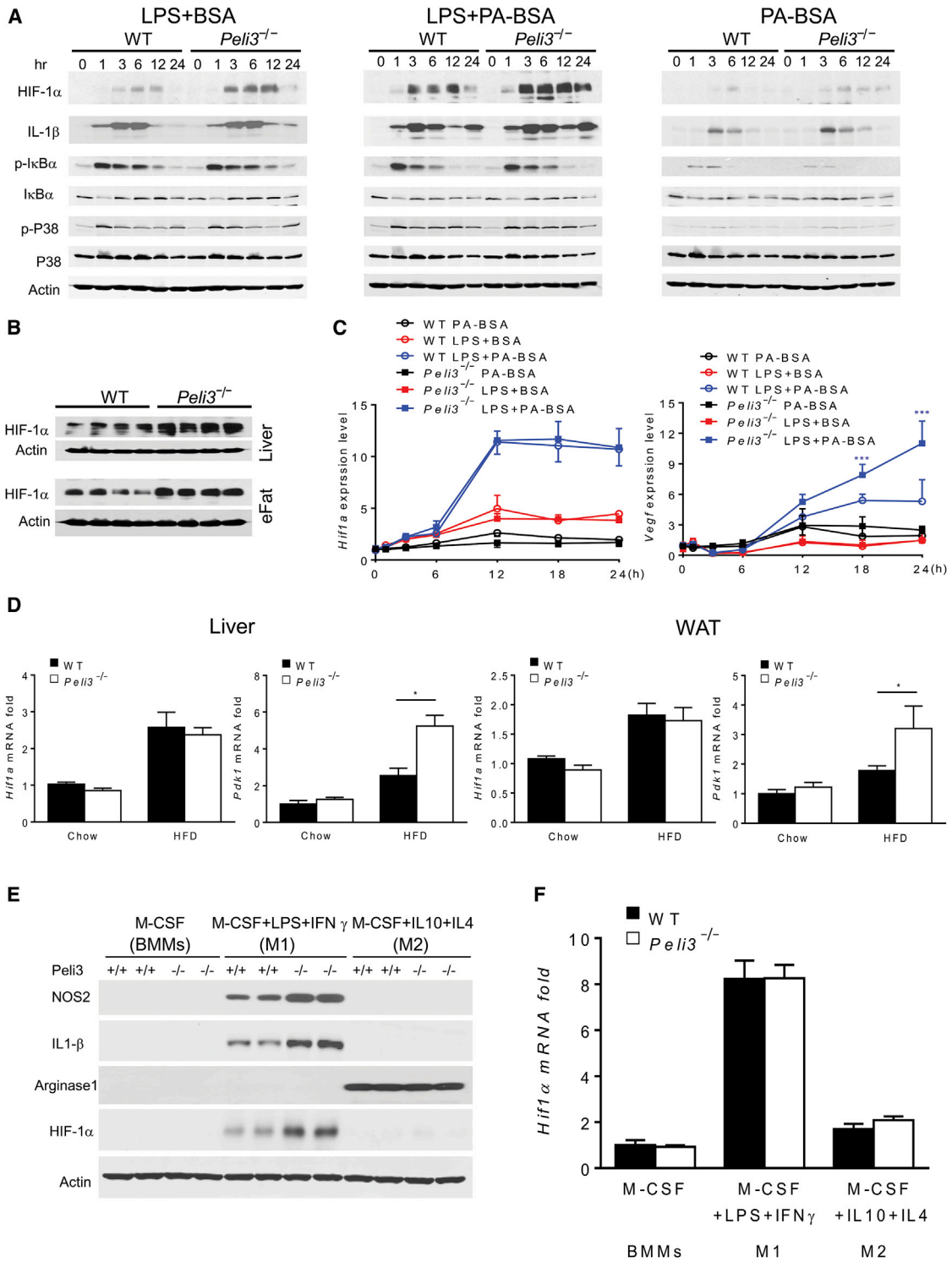

Figure 5. Pellino3 Regulates HIF-1α

(A) Immunoblot analysis of HIF-1α, IL-1β, phosphorylated (p-), and total levels of IκBα and p38 in cell lysates from WT and *Peli3*$^{-/-}$ BMDMs stimulated for 0–24 hr with BSA or PA-BSA in the absence or presence of LPS.

(B) Immunoblot analysis of HIF-1α expression in liver and epididymal fat (eFat) tissue from 7-month-old WT and *Peli3*$^{-/-}$ mice fed a HFD from 2 months old.

(C) Quantitative RT-PCR of mRNA expression for *Hif1a* and *Vegf* in BMDMs isolated from WT and *Peli3*$^{-/-}$ mice and treated for 0–24 hr with BSA or PA-BSA in the absence or presence of LPS.

(D) Quantitative RT-PCR of mRNA expression for *Hif1a* and *Pdk1* in the liver and white adipose tissue (WAT) of 6-month-old wild-type (WT) and *Peli3*$^{-/-}$ mice fed a normal chow diet or HFD from 2 months old (n = 6).

(legend continued on next page)

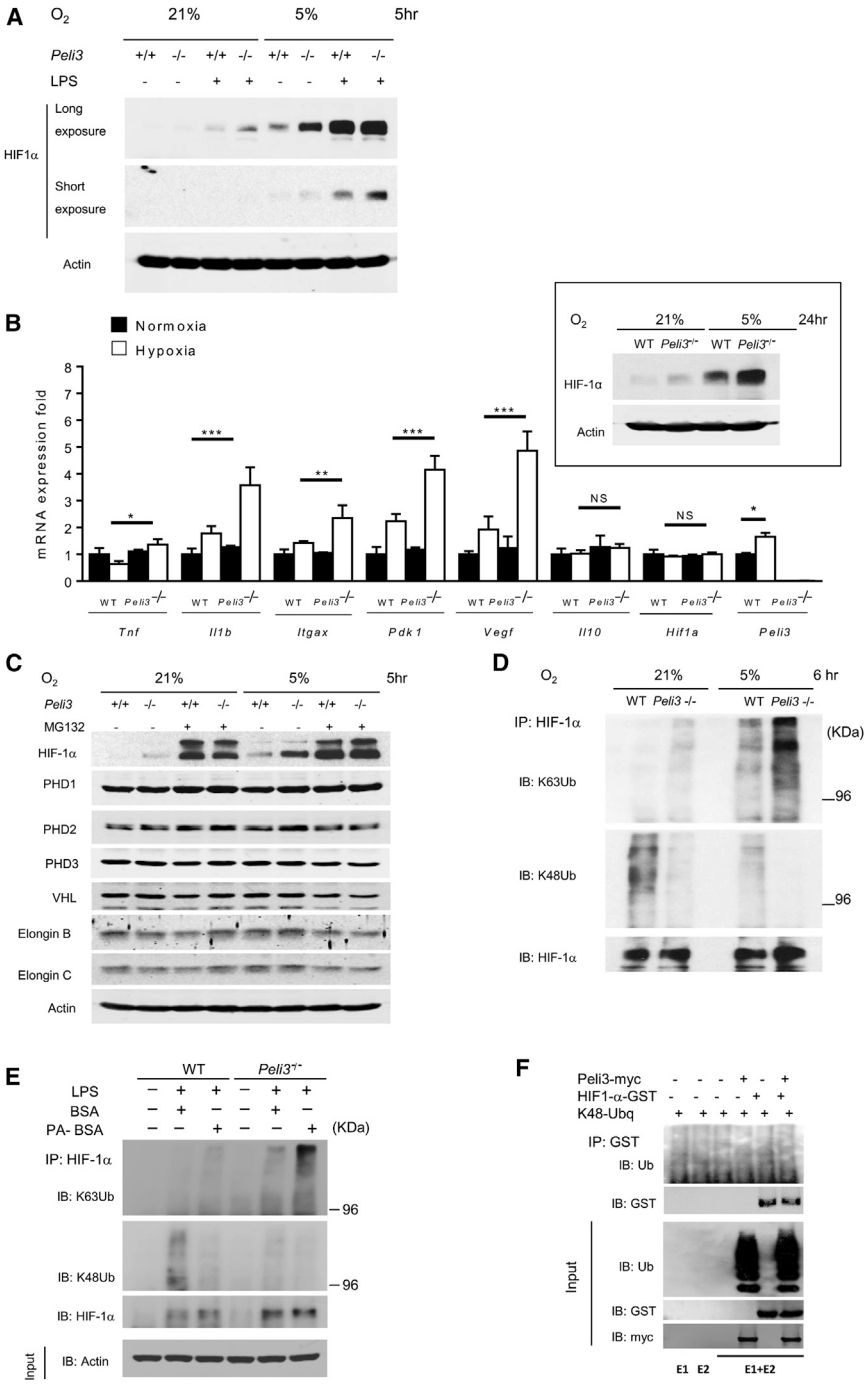

Figure 6. Pellino3 Deficiency Augments Hypoxia-Induced K63-Linked Ubiquitination and Stabilization of HIF-1α and Expression of HIF-1α-Responsive Genes

(A) Immunoblot analysis of HIF-1α expression in WT and *Peli3*$^{-/-}$ BMDMs left untreated or treated with LPS (100 ng/ml) under normoxia (21% O_2) or hypoxia (5% O_2) conditions for 5 hr.

(B) Quantitative PCR of mRNA expression for *Tnf*, *Il1b*, *Itgax*, *Pdk1*, *Vegf*, *Il10*, *HIF-1α*, and *Peli3* in WT and *Peli3*$^{-/-}$ BMDMs incubated under normoxia (21% O_2) or hypoxia (5% O_2) conditions for 24 hr. Data are presented as the mean ± SEM of three independent experiments and were subjected to two-way ANOVA analysis, followed by Bonferroni's multiple-comparison test. *p < 0.05, **p < 0.01, ***p < 0.001; ns, not significant. The inset shows immunoblot analysis of HIF-1α expression in WT and *Peli3*$^{-/-}$ BMDMs incubated in 21% or 5% O_2 for 24 hr.

(C) Immunoblot analysis of HIF-1α, PHD1, PHD2, PHD3, VHL, Elongin B, and Elongin C in WT and *Peli3*$^{-/-}$ BMDMs left untreated or treated with MG132 (20 μm) for 1 hr before 5 hr incubation in 21% or 5% O_2. β-actin was used as a loading control.

(D and E) Immunoblot (IB) analysis of K63-linked ubiquitin, K48-linked ubiquitin, and HIF-1α in immunoprecipitated (IP) HIF-1α samples from WT and *Peli3*$^{-/-}$ BMDMs treated for (D) 6 hr in 21% or 5% O_2 in the presence of MG132 (20 μm) or (E) 7 hr in the absence or presence of LPS with BSA or PA-BSA.

(F) Immunoblot analysis of K48-linked ubiquitin, HIF-1α, and myc (Pellino3) in immunoprecipitated (IP) HIF-1α and lysate (input) samples from in vitro ubiquitination assay.

Data are representative of two to three experiments. See also Figure S6.

Regazzetti et al., 2009). HIF-1α has also been shown to contribute to HFD-induced insulin resistance (Jiang et al., 2011; Kihira et al., 2014; Lee et al., 2014; Shin et al., 2012). The present study provides a plausible signaling framework of such HIF-1α-mediated effects and how hypoxic conditions in adipose tissue can trigger low-level inflammation and ultimately insulin resistance.

Although LPS has recently been shown to elevate succinate concentrations to inhibit prolyl-hydroxylase-mediated hydroxylation of HIF-1α resulting in increased stability of the latter and induction of IL-1β (Tannahill et al., 2013), we now provide evidence for an important signaling axis of TRAF6-HIF-1α-IL-1β that also drives IL-1β expression. Pellino3 is an important negative regulatory of this pathway and acts as a critically important checkpoint to avoid unwanted IL-1β expression. The consequences of removal of this regulatory system is revealed by Pellino3-deficient mice showing exacerbation of HFD-induced inflammation and insulin resistance. Notably in a human context, diabetic obese subjects

(E and F) Immunoblot analysis of NOS2, IL-1β, Arginase 1, HIF-1α, and β-actin (E) and quantitative RT-PCR of mRNA expression for *Hif1a* in M-CSF cultured bone marrow macrophages (BMMs) (F) from WT and *Peli3*$^{-/-}$ mice costimulated with LPS and IFN-γ or IL-4 and IL-10 to generate M1 and M2 populations, respectively. All data are presented as the mean ± SEM of three or four independent experiments and were subjected to two-way ANOVA analysis, followed by Bonferroni's multiple-comparison test. *p < 0.05, ***p < 0.001. See also Figure S5.

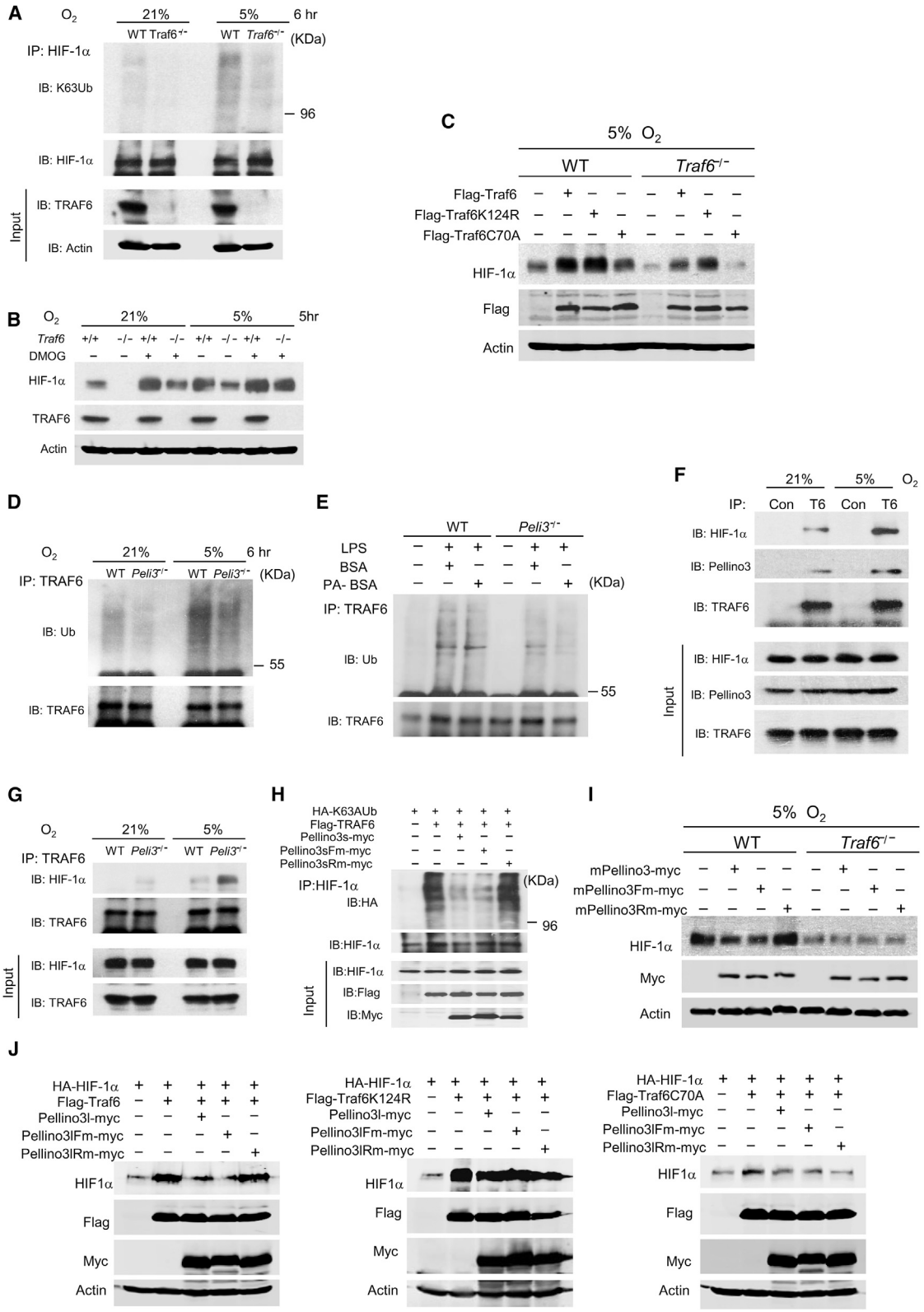

Figure 7. Pellino3 Targets TRAF6 to Negatively Regulate Stabilization of HIF-1α

(A) Immunoblot analysis of K63-linked ubiquitin, HIF-1α, and TRAF6 in immunoprecipitated (IP) HIF-1α and lysate (input) samples from WT and *Traf6*$^{-/-}$ MEFs treated for 6 hr in 21% or 5% O_2 in the presence of MG132 (20 μm).

(legend continued on next page)

show greatly reduced adipose tissue levels of Pellino3. Although the molecular basis to the reduced expression of Pellino3 in obesity remains to be delineated and no polymorphisms or mutations in Pellino3 have yet been identified that associate with insulin resistance or diabetes, the present studies implicate Pellino3 as a molecule with potential protective function in the control of metabolic health.

EXPERIMENTAL PROCEDURES

Mice

Peli3$^{-/-}$ mice were generated on a C57BL/6J background as described (Siednienko et al., 2012; Yang et al., 2013a, 2013b). For diet studies, 8-week-old mice were fed a chow diet (Teklad diet 2918 with 18% calories from fat [Harlan]) or a HFD (Teklad high-fat diet TD.06414 with 60% calories from fat [Harlan]), and had free access to food and water with a 12 hr/12 hr light/dark cycle. For glucose-tolerance tests (GTT), mice were fasted overnight prior to intraperitoneal injection with glucose (1.5 mg/g body weight). Blood glucose levels were measured from whole tail blood with a glucose monitor (Freestyle, Abbott Diabetes Care) at intervals of 0, 15, 30, 60, and 120 min after the glucose injection. For insulin-tolerance tests (ITT), mice were injected intraperitoneally with insulin (1.2 mU/g body weight [Novolin]) after a 5 hr fast and glucose values were measured as above. For IL-1 receptor antagonist (IL-1RA) administration, mice were fed a HFD at 8 weeks old and then injected intraperitoneally with either IL-1RA (10 mg/kg body weight) or endotoxin-free PBS daily, starting at 12 weeks of age, for 12 weeks. Body weights were measured every 2 or 3 weeks. For metabolic measurements, mice were fasted overnight. Blood samples were collected and serum was stored at −20°C until analysis. The insulin levels were determined with an Ultrasensitive Insulin ELISA kit (Crystal CHEM). Triglyceride (TG) levels were measured with a commercial kit (Stanbio Laboratory). For food intake test, mice were individually caged. Food intake was measured weekly. All animal experiments were performed in accordance with the regulations and guidelines of the Irish Department of Health and protocols approved by the Research Ethics committee of National University of Ireland Maynooth.

Analysis of Human Adipose Samples

A total of 20 human subjects (aged 22–66 years) were recruited for this study with all individuals providing written informed consent. The study was approved by the Ethics Committee at St. Vincent's University Hospital (Dublin, Ireland). Half of the subjects were classified as lean (based on mean body mass index [weight (kg)/height (m)^2] of 24.5) and half were categorized as obese (based on mean body mass index of 51.6). Patients with underlying hormone deficiencies, genetic disorders, inflammatory conditions, or occurrences of recent acute infections were excluded. In both groups, 40% of the subjects were male and the mean age of the lean and obese subjects were 49.8 and 43.8 years, respectively. Obese subjects had glycated haemoglobin (HbA1c) levels ranging from 38 to 54 mmol/mol. Omental adipose tissue samples were initially collected into DMEM, supplemented with 10% (v/v) fetal calf serum, from patients undergoing bariatric surgery (obese subjects) or exploratory laparoscopically assisted colonoscopy (lean subjects). Anonymized biopsy samples were stored at −80°C for batch analysis. Frozen biopsy samples were thawed and placed in cell lysis buffer (50 mM Tris-HCl [pH 7.4], containing 150 mM NaCl, 0.5% sodium deoxycholate [w/v], 1% Triton X-100 [v/v], 50 mM NaF, 1 mM Na_3VO_4, 1 mM DTT, 1 mM PMSF, and complete protease-inhibitor "cocktail"), followed by sonication. Cell lysates were centrifuged for 10 min at 14,000 × *g* for removal of cell debris, nuclei, and fat layer. Supernatants were assayed for protein concentration and lysate samples (50 μg) were resolved by SDS-PAGE, transferred to nitrocellulose membranes, and analyzed by immunoblot with anti-Pellino3 (generated in-house). Immunoblot analysis was performed in the absence or presence of the immunogenic peptide that was used to generate the anti-Pellino3, to "define" the nonspecific binding of the antibody. Immunoreactivity was visualized by the Odyssey Imaging System.

In Vitro Polarization of M1 and M2 Macrophages

Tibias and femurs were removed from wild-type and *Peli3*$^{-/-}$ mice by sterile techniques and the bone marrow was flushed with fresh RPMI-1640 medium plus GlutaMAX-I medium. Cells were plated in medium supplemented with M-CSF (25 ng/ml) for 6 days. On day 6, cells were left untreated or were costimulated with LPS (100 ng/ml) and IFN-γ (20 ng/ml) or with IL-4 (25 ng/ml) and IL-10 (10 ng/ml) for 24 hr.

In Vitro Ubiquitination Assay

Recombinant Pellino3 proteins were produced as previously described (Yang et al., 2013a). For the K48 ubiquitination assay, purified recombinant HIF-1α (400 ng) was incubated with a form of ubiquitin containing a single K at residue 48 (K48) (4 μg), E1 (100 nM), UbcH6 (E2) (500 nM), and a protease inhibitor mixture (EDTA-free) in the absence or presence of recombinant Pellino3s (0.5 μg) in 20 mM Tris-HCl (pH 8), containing 2 mM $MgCl_2$, 2 mM ATP, and 100 mM NaCl. Reactions were incubated at 30°C for1.5 hr and terminated by the addition of 1% (w/v) SDS. Samples were heated to 95°C for 5 min to dissociate HIF-1α from any associated proteins and then were diluted 10-fold in lysis buffer (20 mM Tris-HCl [pH 7.4], containing 150 mM NaCl, 1% [vol/vol] Igepal, 10% [wt/vol] glycerol, 50 mM NaF, 1 mM Na_3VO_4, 1 mM dithiothreitol, 1 mM phenylmethylsulfonyl fluoride, and complete protease-inhibitor cocktail [Roche]) before immunoprecipitation and immunoblot analysis.

Statistical Analysis

Prism5 software (GraphPad Software) was used for all statistical tests. A p value of 0.05 was considered significant.

(B) Immunoblot analysis of HIF-1α and TRAF6 in WT and *Traf6*$^{-/-}$ MEFs left untreated or treated with DMOG (200 μm) for 1 hr before 5 hr incubation in 21% or 5% O_2. β-actin was used as a loading control.
(C) Immunoblot analysis of HIF-1α and Flag in WT and *Traf6*$^{-/-}$ MEFs transfected with constructs encoding Flag-tagged wild-type Traf6 or point mutants of Traf6 (K124R, C70A) and exposed to 5% O_2 for 5 hr. β-actin was used as a loading control.
(D and E) Immunoblot (IB) analysis of TRAF6 and ubiquitin in immunoprecipitated (IP) TRAF6 and lysate (input) samples from WT and *Peli3*$^{-/-}$ BMDMs treated for (D) 6 hr in 21% or 5% O_2 in the presence of MG132 (20 μm) or (E) 7 hr with BSA (400 μM) or palmitate conjugated to BSA (PA-BSA) (400 μM) in the absence or presence of LPS (100 ng/ml).
(F) Immunoblot analysis of HIF-1α, Pellino3, and TRAF6 in immunoprecipitated (IP) TRAF6 (T6) and lysate (input) samples from HeLa cells, exposed to 21% or 5% O_2 for 6 hr in the presence of MG132 (20 μm). The controls (Con) represent samples immunoprecipitated with an isotype (IgG) control antibody.
(G) Immunoblot (IB) analysis of TRAF6 and HIF-1α in immunoprecipitated (IP) TRAF6 and lysate (input) samples from WT and *Peli3*$^{-/-}$ BMDMs treated for 6 hr in 21% or 5% O_2 in the presence of MG132 (20 μm).
(H) Immunoblot analysis of HA-ubiqutin, HIF-1α, flag (Traf6), and myc (Pellino3) proteins in immunoprecipitated (IP) HIF-1α and lysate (Input) samples from HEK293T cells previously transfected with constructs encoding HA-tagged K63A ubiquitin (K63AUb; all K residues except K63 mutated to alanine), Flag-tagged Traf6, and myc-tagged Pellino3s and corresponding mutant forms containing mutations in the FHA (Pellino3sFm [R131A, S161A]) and RING domains (Pellino3sRm [C360A, C363A]) and incubated in the presence of MG132 (20 μm) for 3 hr.
(I) Immunoblot analysis of HIF-1α and Myc in WT and *Traf6*$^{-/-}$ MEFs transfected with constructs encoding myc-tagged wild-type mPellino3 or mPellino3 with a mutated FHA (mPellino3Fm) or RING (mPellino3Rm) domain and exposed to 5% O_2 for 5 hr. β-actin was used as a loading control.
(J) Immunoblot analysis of HA-HIF-1α, Flag-tagged Traf6 proteins, and myc-tagged Pellino3 proteins in cell lysates from HEK293T cells previously transfected with constructs encoding HA-HIF-1α, Flag-tagged Traf6 (left) or Traf6 with a mutated K124R (middle) or C70A (right) and myc-tagged Pellino3l and corresponding mutant forms containing mutations in the FHA (Pellino3lFm [R155A, S185A]) and RING domains (Pellino3lRm [C384A, C387A]).
Data are representative of two to three experiments. See also Figure S7.

SUPPLEMENTAL INFORMATION

Supplemental Information includes seven figures and Supplemental Experimental Procedures and can be found with this article online at http://dx.doi.org/10.1016/j.immuni.2014.11.013.

AUTHOR CONTRIBUTIONS

S.Y. developed the concept, designed and performed experiments, analyzed data, prepared the figures, and cowrote the manuscript; B.W. helped develop the concept, designed and performed experiments, and analyzed data; F.H. performed the in vitro K48 ubiquitination assay and HIF-1α stabilization studies; A.E.H. and D.O'S. sourced omental samples from healthy and obese subjects and performed clinical phenotyping of patients; and P.N.M. conceived the study, supervised the overall project, analyzed data, and cowrote the manuscript.

ACKNOWLEDGMENTS

This work was funded by a SFI grant to P.N.M. (12/IA/1736).

Received: May 22, 2014
Accepted: October 9, 2014
Published: December 18, 2014

REFERENCES

Asrih, M., and Jornayvaz, F.R. (2013). Inflammation as a potential link between nonalcoholic fatty liver disease and insulin resistance. J. Endocrinol. *218*, R25–R36.

Baker, R.G., Hayden, M.S., and Ghosh, S. (2011). NF-κB, inflammation, and metabolic disease. Cell Metab. *13*, 11–22.

Böni-Schnetzler, M., and Donath, M.Y. (2013). How biologics targeting the IL-1 system are being considered for the treatment of type 2 diabetes. Br. J. Clin. Pharmacol. *76*, 263–268.

Butler, M.P., Hanly, J.A., and Moynagh, P.N. (2007). Kinase-active interleukin-1 receptor-associated kinases promote polyubiquitination and degradation of the Pellino family: direct evidence for PELLINO proteins being ubiquitin-protein isopeptide ligases. J. Biol. Chem. *282*, 29729–29737.

Chang, M., Jin, W., and Sun, S.C. (2009). Peli1 facilitates TRIF-dependent Toll-like receptor signaling and proinflammatory cytokine production. Nat. Immunol. *10*, 1089–1095.

Chang, M., Jin, W., Chang, J.H., Xiao, Y., Brittain, G.C., Yu, J., Zhou, X., Wang, Y.H., Cheng, X., Li, P., et al. (2011). The ubiquitin ligase Peli1 negatively regulates T cell activation and prevents autoimmunity. Nat. Immunol. *12*, 1002–1009.

Fujisaka, S., Usui, I., Bukhari, A., Ikutani, M., Oya, T., Kanatani, Y., Tsuneyama, K., Nagai, Y., Takatsu, K., Urakaze, M., et al. (2009). Regulatory mechanisms for adipose tissue M1 and M2 macrophages in diet-induced obese mice. Diabetes *58*, 2574–2582.

Fujisaka, S., Usui, I., Ikutani, M., Aminuddin, A., Takikawa, A., Tsuneyama, K., Mahmood, A., Goda, N., Nagai, Y., Takatsu, K., and Tobe, K. (2013). Adipose tissue hypoxia induces inflammatory M1 polarity of macrophages in an HIF-1α-dependent and HIF-1α-independent manner in obese mice. Diabetologia *56*, 1403–1412.

Goh, E.T., Arthur, J.S., Cheung, P.C., Akira, S., Toth, R., and Cohen, P. (2012). Identification of the protein kinases that activate the E3 ubiquitin ligase Pellino 1 in the innate immune system. Biochem. J. *441*, 339–346.

Gregor, M.F., and Hotamisligil, G.S. (2011). Inflammatory mechanisms in obesity. Annu. Rev. Immunol. *29*, 415–445.

Hodson, L. (2014). Adipose tissue oxygenation: effects on metabolic function. Adipocyte *3*, 75–80.

Item, F., and Konrad, D. (2012). Visceral fat and metabolic inflammation: the portal theory revisited. Obes. Rev. *13* (2), 30–39.

Jaakkola, P., Mole, D.R., Tian, Y.M., Wilson, M.I., Gielbert, J., Gaskell, S.J., von Kriegsheim, A., Hebestreit, H.F., Mukherji, M., Schofield, C.J., et al. (2001). Targeting of HIF-alpha to the von Hippel-Lindau ubiquitylation complex by O2-regulated prolyl hydroxylation. Science *292*, 468–472.

Jiang, C., Qu, A., Matsubara, T., Chanturiya, T., Jou, W., Gavrilova, O., Shah, Y.M., and Gonzalez, F.J. (2011). Disruption of hypoxia-inducible factor 1 in adipocytes improves insulin sensitivity and decreases adiposity in high-fat diet-fed mice. Diabetes *60*, 2484–2495.

Jin, C., Henao-Mejia, J., and Flavell, R.A. (2013). Innate immune receptors: key regulators of metabolic disease progression. Cell Metab. *17*, 873–882.

Kihira, Y., Miyake, M., Hirata, M., Hoshina, Y., Kato, K., Shirakawa, H., Sakaue, H., Yamano, N., Izawa-Ishizawa, Y., Ishizawa, K., et al. (2014). Deletion of hypoxia-inducible factor-1α in adipocytes enhances glucagon-like peptide-1 secretion and reduces adipose tissue inflammation. PLoS ONE *9*, e93856.

Könner, A.C., and Brüning, J.C. (2011). Toll-like receptors: linking inflammation to metabolism. Trends Endocrinol. Metab. *22*, 16–23.

Lee, Y.S., Kim, J.W., Osborne, O., Oh, Y., Sasik, R., Schenk, S., Chen, A., Chung, H., Murphy, A., Watkins, S.M., et al. (2014). Increased adipocyte O2 consumption triggers HIF-1α, causing inflammation and insulin resistance in obesity. Cell *157*, 1339–1352.

Lin, C.C., Huoh, Y.S., Schmitz, K.R., Jensen, L.E., and Ferguson, K.M. (2008). Pellino proteins contain a cryptic FHA domain that mediates interaction with phosphorylated IRAK1. Structure *16*, 1806–1816.

Lumeng, C.N., Bodzin, J.L., and Saltiel, A.R. (2007). Obesity induces a phenotypic switch in adipose tissue macrophage polarization. J. Clin. Invest. *117*, 175–184.

Lumeng, C.N., DelProposto, J.B., Westcott, D.J., and Saltiel, A.R. (2008). Phenotypic switching of adipose tissue macrophages with obesity is generated by spatiotemporal differences in macrophage subtypes. Diabetes *57*, 3239–3246.

Martinon, F., Burns, K., and Tschopp, J. (2002). The inflammasome: a molecular platform triggering activation of inflammatory caspases and processing of proIL-beta. Mol. Cell *10*, 417–426.

Matsuzawa, Y., Shimomura, I., Nakamura, T., Keno, Y., Kotani, K., and Tokunaga, K. (1995). Pathophysiology and pathogenesis of visceral fat obesity. Obes. Res. *3* (2), 187S–194S.

Moynagh, P.N. (2011). Peli1 (rel)ieves autoimmunity. Nat. Immunol. *12*, 927–929.

Moynagh, P.N. (2014). The roles of Pellino E3 ubiquitin ligases in immunity. Nat. Rev. Immunol. *14*, 122–131.

Nguyen, M.T., Favelyukis, S., Nguyen, A.K., Reichart, D., Scott, P.A., Jenn, A., Liu-Bryan, R., Glass, C.K., Neels, J.G., and Olefsky, J.M. (2007). A subpopulation of macrophages infiltrates hypertrophic adipose tissue and is activated by free fatty acids via Toll-like receptors 2 and 4 and JNK-dependent pathways. J. Biol. Chem. *282*, 35279–35292.

Ohh, M., Park, C.W., Ivan, M., Hoffman, M.A., Kim, T.Y., Huang, L.E., Pavletich, N., Chau, V., and Kaelin, W.G. (2000). Ubiquitination of hypoxia-inducible factor requires direct binding to the beta-domain of the von Hippel-Lindau protein. Nat. Cell Biol. *2*, 423–427.

Ordureau, A., Smith, H., Windheim, M., Peggie, M., Carrick, E., Morrice, N., and Cohen, P. (2008). The IRAK-catalysed activation of the E3 ligase function of Pellino isoforms induces the Lys63-linked polyubiquitination of IRAK1. Biochem. J. *409*, 43–52.

Poggi, M., Bastelica, D., Gual, P., Iglesias, M.A., Gremeaux, T., Knauf, C., Peiretti, F., Verdier, M., Juhan-Vague, I., Tanti, J.F., et al. (2007). C3H/HeJ mice carrying a toll-like receptor 4 mutation are protected against the development of insulin resistance in white adipose tissue in response to a high-fat diet. Diabetologia *50*, 1267–1276.

Regazzetti, C., Peraldi, P., Grémeaux, T., Najem-Lendom, R., Ben-Sahra, I., Cormont, M., Bost, F., Le Marchand-Brustel, Y., Tanti, J.F., and Giorgetti-Peraldi, S. (2009). Hypoxia decreases insulin signaling pathways in adipocytes. Diabetes *58*, 95–103.

Schauvliege, R., Janssens, S., and Beyaert, R. (2006). Pellino proteins are more than scaffold proteins in TLR/IL-1R signalling: a role as novel RING E3-ubiquitin-ligases. FEBS Lett. *580*, 4697–4702.

Schauvliege, R., Janssens, S., and Beyaert, R. (2007). Pellino proteins: novel players in TLR and IL-1R signalling. J. Cell. Mol. Med. *11*, 453–461.

Shin, M.K., Drager, L.F., Yao, Q., Bevans-Fonti, S., Yoo, D.Y., Jun, J.C., Aja, S., Bhanot, S., and Polotsky, V.Y. (2012). Metabolic consequences of high-fat diet are attenuated by suppression of HIF-1α. PLoS ONE *7*, e46562.

Siednienko, J., Jackson, R., Mellett, M., Delagic, N., Yang, S., Wang, B., Tang, L.S., Callanan, J.J., Mahon, B.P., and Moynagh, P.N. (2012). Pellino3 targets the IRF7 pathway and facilitates autoregulation of TLR3- and viral-induced expression of type I interferons. Nat. Immunol. *13*, 1055–1062.

Skeldon, A.M., Faraj, M., and Saleh, M. (2014). Caspases and inflammasomes in metabolic inflammation. Immunol. Cell Biol. *92*, 304–313.

Smith, H., Peggie, M., Campbell, D.G., Vandermoere, F., Carrick, E., and Cohen, P. (2009). Identification of the phosphorylation sites on the E3 ubiquitin ligase Pellino that are critical for activation by IRAK1 and IRAK4. Proc. Natl. Acad. Sci. USA *106*, 4584–4590.

Smith, H., Liu, X.Y., Dai, L., Goh, E.T., Chan, A.T., Xi, J., Seh, C.C., Qureshi, I.A., Lescar, J., Ruedl, C., et al. (2011). The role of TBK1 and IKKε in the expression and activation of Pellino 1. Biochem. J. *434*, 537–548.

Strelow, A., Kollewe, C., and Wesche, H. (2003). Characterization of Pellino2, a substrate of IRAK1 and IRAK4. FEBS Lett. *547*, 157–161.

Sun, H., Li, X.B., Meng, Y., Fan, L., Li, M., and Fang, J. (2013). TRAF6 upregulates expression of HIF-1α and promotes tumor angiogenesis. Cancer Res. *73*, 4950–4959.

Tack, C.J., Stienstra, R., Joosten, L.A., and Netea, M.G. (2012). Inflammation links excess fat to insulin resistance: the role of the interleukin-1 family. Immunol. Rev. *249*, 239–252.

Takeda, N., O'Dea, E.L., Doedens, A., Kim, J.W., Weidemann, A., Stockmann, C., Asagiri, M., Simon, M.C., Hoffmann, A., and Johnson, R.S. (2010). Differential activation and antagonistic function of HIF-alpha isoforms in macrophages are essential for NO homeostasis. Genes Dev. *24*, 491–501.

Tannahill, G.M., Curtis, A.M., Adamik, J., Palsson-McDermott, E.M., McGettrick, A.F., Goel, G., Frezza, C., Bernard, N.J., Kelly, B., Foley, N.H., et al. (2013). Succinate is an inflammatory signal that induces IL-1β through HIF-1α. Nature *496*, 238–242.

Tsukumo, D.M., Carvalho-Filho, M.A., Carvalheira, J.B., Prada, P.O., Hirabara, S.M., Schenka, A.A., Araújo, E.P., Vassallo, J., Curi, R., Velloso, L.A., and Saad, M.J. (2007). Loss-of-function mutation in Toll-like receptor 4 prevents diet-induced obesity and insulin resistance. Diabetes *56*, 1986–1998.

Wen, H., Gris, D., Lei, Y., Jha, S., Zhang, L., Huang, M.T., Brickey, W.J., and Ting, J.P. (2011). Fatty acid-induced NLRP3-ASC inflammasome activation interferes with insulin signaling. Nat. Immunol. *12*, 408–415.

Xiao, Y., Jin, J., Chang, M., Chang, J.H., Hu, H., Zhou, X., Brittain, G.C., Stansberg, C., Torkildsen, Ø., Wang, X., et al. (2013). Peli1 promotes microglia-mediated CNS inflammation by regulating Traf3 degradation. Nat. Med. *19*, 595–602.

Xu, H., Barnes, G.T., Yang, Q., Tan, G., Yang, D., Chou, C.J., Sole, J., Nichols, A., Ross, J.S., Tartaglia, L.A., and Chen, H. (2003). Chronic inflammation in fat plays a crucial role in the development of obesity-related insulin resistance. J. Clin. Invest. *112*, 1821–1830.

Yang, S., Wang, B., Humphries, F., Jackson, R., Healy, M.E., Bergin, R., Aviello, G., Hall, B., McNamara, D., Darby, T., et al. (2013a). Pellino3 ubiquitinates RIP2 and mediates Nod2-induced signaling and protective effects in colitis. Nat. Immunol. *14*, 927–936.

Yang, S., Wang, B., Tang, L.S., Siednienko, J., Callanan, J.J., and Moynagh, P.N. (2013b). Pellino3 targets RIP1 and regulates the pro-apoptotic effects of TNF-α. Nat. Commun. *4*, 2583.